Inquiro, the UAB undergraduate science research journal

Volume 2013 | Number 7 Article 22

2013

Method for the determination of trajectory angles of directional secretory vesicles in cultured astrocytes

Chapin E. Cavender

Manoj K. Gottipati

Eric B. Malarkey

Vladimir Parpura

Method for the determination of trajectory angles of directional secretory vesicles in cultured astrocytes

Chapin E. Cavender[1], Manoj K. Gottipati[1], Erik B. Malarkey[1,2], and Vladimir Parpura[1,3]

[1] Department of Neurobiology, University of Alabama at Birmingham, [2] Department of Cell, Developmental, and Integrative Biology, University of Alabama at Birmingham
[3] Department of Biotechnology, University of Rijeka, Rijeka, Croatia.

Abstract

Astrocytes provide a principal pathway for glutamate uptake in the mammalian brain, a task accomplished by the powerful action of excitatory amino acid transporters (EAAT) 1 and 2. These transporters are synthesized within the endoplasmic reticulum and are then trafficked to the plasma membrane. The characteristics of their intracellular traffic within astrocytes have not been investigated. We monitored the trafficking of secretory vesicles laden with the recombinant fluorescent protein chimera of EAAT2 in cultured astrocytes. Such vesicles appeared as fluorescent puncta, and their trafficking parameters were obtained using original algorithms, which we describe here in detail. We determined the maximal displacement, average instantaneous speed, and trajectory angle of individual puncta/vesicles, with angles near 0° indicating radial movement directly away from or toward the nucleus and angles near 90° indicating tangential movement. Analysis of these trafficking parameters demonstrated that trafficking of EAAT2-laden vesicles has typical characteristics expected of the trafficking of secretory vesicles in cultured astrocytes. The distribution of trajectory angles for directional vesicles, i.e. those with a maximal displacement greater than 1 μm within the 40-s time-lapse imaging, was found to be unimodal, with angles near 0° being the most prominent (mode 7°). These measurements are in good agreement with previous measurements of trajectory angles of similar trafficking vesicles carrying cannabinoid receptor 1, evidencing the validity and robustness of our analytical approach and algorithms.

Introduction

Research in the past two decades has shown that astrocytes, a type of glial cell and the most numerous cell in the mammalian brain, have central roles in the structural and functional development and homeostasis of the nervous system.[1-2] One of these roles is to remove excess neurotransmitter molecules from the extracellular space, particularly in the vicinity of synaptic sites. While neurotransmitters mediate typical signaling between neural cells, excessive buildup of these molecules outside of the cells can have deleterious consequences. For example, the major excitatory amino acid neurotransmitter glutamate can cause neuronal death when present in high concentrations in the extracellular space. This condition is known as excitotoxicity and has been implicated in the progression of neurodegenerative diseases such as Alzheimer's disease.[3]

Astrocytes provide a principal pathway for the uptake of glutamate. About 80% of all glutamate released during synaptic transmission is taken up by astroglial cells, while most of the remaining 20% is taken up by post-synaptic neurons.[4-5] This uptake of glutamate by mature astrocytes is accomplished by the plasma membrane sodium-dependent excitatory amino acid transporter 2 (EAAT2). This membrane protein is trafficked by secretory vesicles from the endoplasmic reticulum to the plasma membrane along tracts in the cytoskeleton. In addition to ubiquitous actin- and microtubule-based mechanisms for vesicle trafficking, astrocytes exhibit trafficking mechanisms dependent on the intermediate filament proteins glial fibrillary acidic protein and vimentin.[6-7]

Previous analysis has yielded two categories of trafficking vesicles in astrocytes. These are distinguished by the magnitude of the vesicles' maximal displacement, the greatest distance between any two points on the vesicle's trajectory, within a specified time interval.[7-9] For the lengths of those experiments (15 s or 40 s), non-directional vesicles have a maximal displacement less than 1 μm, and their motion is governed by simple diffusion; directional vesicles have a maximal displacement greater than 1 μm, and their motion is more complex.

One parameter associated with vesicle trafficking that has not been studied extensively is the trajectory angle, defined as the angle between the trajectory of a vesicle and a vector in the radial direction away from the nucleus of the cell (see materials and methods and Figure 1).[9] This parameter is useful for defining a preferred direction of motion for the directional vesicles. Indeed, it has been instrumental in discovering a preference for radial trafficking (motion directly toward or away from the nucleus) of vesicles carrying fluorescently tagged cannabinoid receptor 1 (CB1R) in rat astrocytes,[9] as evident from detecting a mode near 0° for a unimodal distribution of angles. Consequently, the goal of this article

is to describe a method for determining the trajectory angles of directional vesicles. This method utilizes a custom-written Visual Basic routine for Microsoft® Excel, referred to in the present study as a custom script.

Trafficking of fluorescently tagged EAAT2 vesicles in cultured mouse cortical astrocytes was studied, and the results were compared to those of previous trafficking studies. Overall, the EAAT2-laden vesicles display preferential radial trajectories.

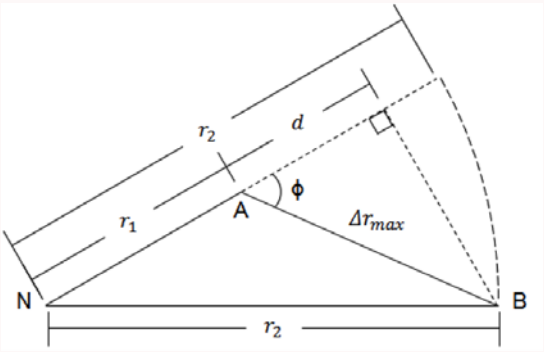

Figure 1. Geometry of vesicular trafficking. The centroid of the nucleus is located at vertex N. The vector representing maximal displacement of a vesicle/punctum is defined by the endpoints A and B. r_1 represents the distance between the centroid of the nucleus and the earlier endpoint (point A) of the maximal displacement vector, and r_2 represents the distance between the centroid of the nucleus and the later endpoint (point B) of the maximal displacement vector. The dashed curve represents the rotation of the vector ***NB*** *around an axis through N perpendicular to the page to assist in the visualization of the distances r_2 and r_1. The angle marked ϕ is the angle between the radial vector* ***NA*** *and the maximal displacement vector* $\boldsymbol{\Delta r_{max}}$.

Materials and methods

Purified astrocytic cell culture

Purified astrocytic cultures were made as described elsewhere.[10-11] Visual cortices from 0- to 2- day-old C57BL/6 mice pups were isolated and treated with papain (20 I.U./mL; Sigma-Aldrich, Sr. Louis, MO) in the presence of L-cysteine (0.2 mg/mL) for 1 hour at 37 °C. Cortices were treated with trypsin inhibitor (type II-O, 10 mg/mL; Sigma-Aldrich) for 5 minutes at room temperature to neutralize the enzymatic activity of papain and then triturated in cell culture media using a glass serological pipette until no visible clumps appeared. The resulting cell suspension was plated into 25 cm^2 tissue culture flasks and left for 1 hour at 37 °C in a 95% air / 5% CO_2 incubator to allow for cell attachment, after which the flasks were washed with Hank's balanced salt solution (HBSS). The HBSS was replaced with cell culture media containing α-minimum essential medium (without phenol red; Invitrogen™, Life technologies Corp., Grand Island, NY) supplemented with fetal bovine serum (10% v/v, HyClone™, Thermo Fisher Scientific Inc., Waltham, MA), sodium bicarbonate (14 mM), sodium pyruvate (1 mM), D-glucose (20 mM), L-glutamine (2 mM), penicillin (100 I.U./mL), and streptomycin (100 µg/mL) (pH 7.35). The flasks were returned to the incubator and the cells were allowed to grow and proliferate for 10 to 14 days to reach approximately 60% confluency, after which the flasks were purified for astrocytes using a previously described procedure.[12] The flasks were washed with ice cold culture media to kill the neurons and side-tapped to detach the microglia, dead neurons, and debris. The flasks were then shaken twice on a horizontal orbital shaker at 37 °C and 260 rpm, first for 1.5 hours followed by two exchanges with ice cold cell culture media and again for 18 hours. At this juncture, purified astrocytes attached to the flask were detached using trypsin (10 000 N_α-benzoyl-L-arginine ethyl ester hydrochloride units/mL; Invitrogen™) diluted in HBSS for 2 to 3 minutes and pelleted by centrifugation for 10 minutes at 100 x *g*. The pellet was resuspended in cell culture media, plated onto round glass coverslips (12 mm in diameter) coated with polyethyleneimine (PEI, 1 mg/mL),[13] inlayed in plastic tissue culture dishes (round, 35 mm in diameter) containing 4 segments—each segment receiving one coverslip—and returned to the incubator for 1 hour, after which the cell suspension was replaced with cell culture media.

Transfection

The cells were transfected one day after plating with an EAAT2-EGFP plasmid (kindly provided by Dr. Jeffrey D. Rothstein, The Johns Hopkins University, Baltimore, MD) encoding EAAT2 tagged at its C-terminus with the enhanced green fluorescent protein (EGFP). Each dish received 1 µg of the plasmid and 2 µL of TransIT-293 (Mirus Bio, LLC, Madison, WI), premixed as per manufacturer's instructions. Four hours after transfection, the dishes were washed with HBSS, which was replaced with fresh culture media, and the dishes were returned to the incubator for 3 days until used in experiments.

Image acquisition

Coverslips (thickness #1, 0.13-0.16 mm, refractive index 1.5255 at λ = 564 nm and 20 °C; D-263 borosilicate glass, Erie Scientific Company; purchased via Fisher Scientific, cat. no. 12-545-82-12CIR-1D) containing cultured astrocytes were mounted onto an imaging chamber filled with an aqueous external solution (pH 7.4) consisting of sodium chloride (140 mM), potassium chloride (5 mM), calcium chloride (2 mM), magnesium chloride (2mM), D-glucose (5 mM), and HEPES (10 mM) at 20 °C - 24 °C and standard atmospheric pressure. An inverted microscope equipped with differential interference contrast (DIC; halogen lamp, 100 W) and wide-field epifluorescence illumination (xenon arc lamp, 100 W) was used with a standard fluorescein isothiocyanate (FITC) filter set (excitation 480/30x nm, dichroic 505DCXR and emission 535/40 nm), a 60x Plan Apochromatic objective lens (numerical aperture, 1.4), and Nikon Type A immersion

oil (refractive index 1.515 at 23 °C) to visualize the cells expressing EAAT2-EGFP. DIC imaging was used to visualize the cell nuclei. The Rayleigh transverse and axial resolutions of the objective were calculated to be 233 nm and 833 nm, respectively, at the 535-nm emission wavelength. Still images and time-lapse images were acquired using a CoolSNAP®-HQ cooled charge coupled device camera (Photometrics, Tucson, AZ) with an exposure time of 500 ms and MetaMorph® 6.1 software (Molecular Devices, Chicago, IL). One pixel corresponds to a square with 104.7-nm sides.

Vesicle trafficking

Trafficking of intracellular vesicles (appearing as intracellular fluorescent puncta) was performed using MetaMorph® imaging software. Time-lapse images of individual cells taken at 1.2 frames s^{-1} for 40 s were filtered using a smoothing kernel—referred to as background flattening in MetaMorph®—to accentuate the edges, resulting in false shading images. Subsequently, an intensity threshold was applied to these images. At this juncture, puncta, whose edge intensities exceeded the set threshold value and whose area was between 4 and 70 pixels, were selected for analysis, and the coordinates of their centroids were obtained in each frame. Of note, an apparent fluorescent punctum size exceeds that of the physical object studied, i.e. a trafficking vesicle, which in astrocytes is reported to be approximately 300 nm in diameter in live astrocytes.[14] For brevity, we shall refer to the coordinates of the centroid of a punctum as the position of the punctum. Puncta located fewer than 10 pixels (approximately 1 μm) from the lateral plasma membrane, puncta that could not be tracked in every frame, and puncta whose paths intersected those of other puncta were excluded from the analysis. Trafficking data for each punctum was analyzed using a custom Visual Basic script in Microsoft® Excel. The script calculated the maximal displacement, average instantaneous speed (the average of the speeds of the punctum for each time step), and trajectory angle for each punctum and plotted the trajectory of the punctum with respect to the centroid of the nucleus. To obtain the centroid of the nucleus, we first hand-traced the outline of the nuclear region based on the DIC image of the cell, which was further used to obtain the centroid using ImageJ software 1.47 (NIH, Washington, DC).

Determination of trajectory angles

Let N be the point representing the coordinates of the centroid of the nucleus, and let A and B be the endpoints of the vector representing the maximal displacement of a directional punctum (Figure 1). Also, let r_1 represent the distance between points N and A, and let r_2 represent the distance between points N and B. Then, the angle ϕ between the radial vector **NA** and the maximal displacement vector $\Delta \mathbf{r}_{max}$ is given by

$$\phi = \arccos\left(\frac{d}{\Delta r_{\max}}\right) \qquad (1)$$

If the distance between the punctum and the nucleus centroid is much greater than the maximal displacement, i.e. $r_1 \gg r_2$, then $d \approx r_2 - r_1$. In such a case, the expression for ϕ can be written as

$$\phi = \arccos\left(\frac{r_2 - r_1}{\Delta r_{\max}}\right) \qquad (2)$$

Since the trajectory angle must fall between +90° and −90°, we define the trajectory angle using the following expression:

$$\theta = \arccos\left(\left|\frac{r_2 - r_1}{\Delta r_{\max}}\right|\right) \qquad (3)$$

We assign positive angles to the vesicles moving away from the nucleus and negative angles to the vesicles moving toward the nucleus. Thus, vesicles which move directly away from or toward the centroid of the nucleus have trajectory angles of ±0°, respectively, and vesicles which move in a tangential direction with respect to the centroid of the nucleus have trajectory angles of ±90°. The sign of the trajectory angle was determined by comparing the coordinates of the endpoints of the maximal displacement and the frames in which the punctum was positioned at those endpoints. If the x-coordinate of one endpoint was exactly equal to that of the other endpoint, the custom script threw an error and the punctum (1 of 1111 studied) was excluded from angle analysis.

Results

Astrocytes expressing EAAT2-EGFP displayed bright fluorescent puncta throughout the cell, with an apparent greater density of puncta in peripheral areas (Figure 2A), which are thinner than 1 μm and are well suited for vesicular tracking.[8-9,15] Once an astrocyte of interest was located based on its fluorescence, we acquired a corresponding DIC image of the cell. This image was used to obtain the coordinates of the centroid of the nucleus (Figure 2B). Trafficking of intracellular vesicles/puncta was performed on time-lapse images, lasting 40 s, of individual astrocytes. Each image frame was kernel-smoothened to obtain the corresponding false shading images (Figure 2C), to which we applied an operative threshold value to define putative puncta (Figure 2D, orange). The trajectories of the puncta whose edge intensities exceeded the threshold value and whose areas were between 4 and 70 pixels were determined (Figure 2D); for additional exclusion criteria, consult materials and methods.

Mobility was characterized by calculating the maximal displacement, average instantaneous speed, and trajectory angle for each punctum. Puncta whose maximal displacement

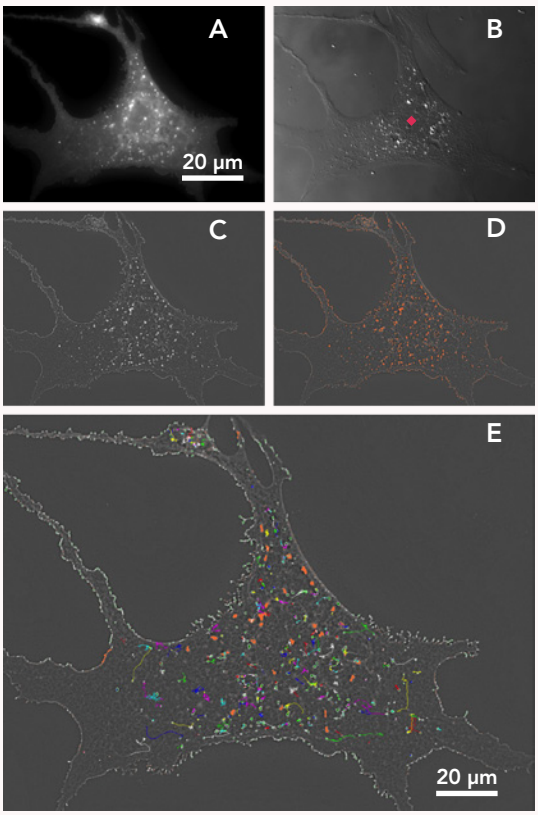

Figure 2. Visualization of EAAT2-EGFP vesicles in cultured astrocytes. (A) A typical astrocyte imaged using a FITC filter set to visualize the fluorescent puncta. (B) The cell shown in A imaged under DIC to disclose the nucleus. The red rhombus is positioned at the centroid of the nucleus. (C) Fluorescence image shown in A kernel-smoothened to obtain a false shading image. (D) An operative intensity threshold applied to the image shown in C. Puncta whose edge fluorescence intensities exceeded the threshold were identified (orange). (E) Composite motility of puncta from the 40-s time-lapse acquisition. Colored curves (other than orange) are overlaid on the false shading image to show the trajectories of the puncta within the astrocyte.

was less than 1 µm were classified as non-directional, and puncta whose maximal displacement exceeded 1 µm were classified as directional, as this distance is larger than the greatest distance which can be traveled by an average-sized secretory vesicle in 40 s under the influence of simple diffusion.[8-9] Examples of typical trajectories for non-directional and directional puncta are shown in Figure 3A. The majority of vesicles analyzed (57%; 1482 of 2593 tracked puncta from 15 astrocytes) were classified as non-directional based on their maximal displacement (Figure 3B). The distributions of average instantaneous speeds for non-directional and directional puncta were non-normal (D'Agostino test, D' = 15066.7 and 9839.2, respectively; both $p < 0.01$). The distributions were analyzed using non-parametric statistics, and, as expected, the average instantaneous speed of directional puncta was significantly greater than that of non-directional puncta (median values of 0.142 µm/s and 0.052 µm/s, respectively; Figure 3C; Mann-Whitney U-test, $p < 0.0001$). Trajectory angles were determined for directional puncta using the method described above (Figure 3D). One punctum out of 1111 was excluded from angle analysis (see materials and methods). The distribution of trajectory angles of EAAT2-EGFP puncta was non-normal (D'Agostino test, D' = 10675.3, $p < 0.01$). However, the distribution of angles was found to be unimodal (Hartigan's dip test, $D(F_{1110}) = 0.0071$, $p > 0.05$) with angles near 0° being the most prominent (mode 7°).

Discussion

The trafficking parameters analyzed here for EAAT2-EGFP puncta compare favorably to the measurements obtained for astrocytic vesicles in similar studies. The greater proportion of non-directional vesicles (whose movement is due to diffusion) over directional vesicles (whose movement is due to active transport mechanisms) is consistent with the results from studies of trafficking of atrial natriuretic peptide vesicles[6,8] and of CB1R vesicle;[9] the directional vesicles are known to interact with actin filaments, microtubule filaments, and intermediate filaments.[6,8] Furthermore, the greater instantaneous speed of directional vesicles over non-directional vesicles is consistent with the results from the study of trafficking of CB1R vesicles.[9] Thus, movement of EAAT2 vesicles is characterized as typical of vesicular trafficking in cultured astrocytes.

The unimodality of the distribution of trajectory angles for directional puncta and the prominence of angles near 0° corroborates with the previous analysis of trajectory angles in CB1R vesicles.[9] From the consistency of these results with the previous analyses, we conclude that the method described above for determining the trajectory angles of directional vesicles is valid under the restriction that the maximal displacement of vesicles analyzed must not be on the same order of magnitude as the distance of the vesicle from the centroid of the nucleus, which is unlikely due to the size of the nucleus. Further analysis is needed to determine how large the maximal displacement needs to be with respect to the distance from the centroid of the nucleus in order to introduce noticeable error into the approximation. Although some error may be introduced by the analysis in two dimensions of vesicles that move in three dimensions, the thin areas (approximately 1 µm) of cultured astrocytes used for analysis greatly limit the motion of vesicles in the direction perpendicular to the imaging plane. Thus, this motion is unlikely to significantly affect the measurement of punctum mobility.[8] Future research concerning vesicular trafficking will utilize the method described here to characterize the trajectories of secretory vesicles in cultured astrocytes. Possible applications include methods for increasing the trafficking of EAAT2 vesicles in astrocytes, i.e. delivery of these transporters to the plasma membrane, as a means to increase the uptake of glutamate and reduce excitotoxicity.

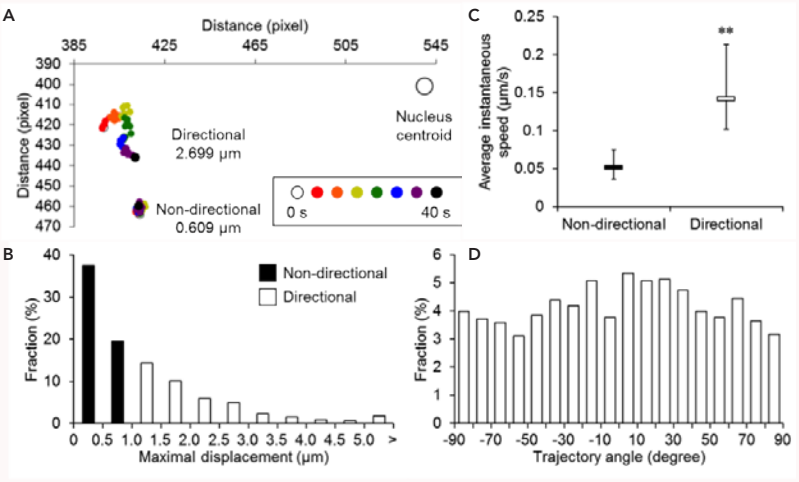

Figure 3. Trafficking parameters for EAAT2-EGFP vesicles in cultured astrocytes. (A) Examples of typical trajectories of non-directional (lower cluster, maximal displacement 0.609 µm) and directional (upper cluster, maximal displacement 2.699 µm) puncta. Trajectories are color-coded by time (color-coding shown in the inset). The position of the centroid of the nucleus is represented by the large open circle (top right corner, not to scale). (B) Frequency of maximal displacements of puncta as a percentage of all puncta (n = 2593) from 15 astrocytes. Non-directional puncta (maximal displacement less than 1 µm) and directional puncta (maximal displacement greater than 1 µm) are marked. (C) Comparison of instantaneous speeds of directional puncta (n = 1111) to those of significantly slower non-directional puncta (n = 1482) (Mann-Whitney U-test, $p < 0.0001$). Boxes represent median values ± interquartile range. (D) Frequency of trajectory angles of directional puncta as a percentage of all directional puncta for which trajectory angles could be calculated (n = 1110; see materials and methods) from 15 cells. The distribution was determined to be unimodal (Hartigan's dip test, $p > 0.05$) with angles near 0° being the most prominent. The black arrowhead indicates the mode for the distribution (7°).

Acknowledgements

We would like to thank Dr. Jeffrey D. Rothstein for kindly providing us with the EAAT2-EGFP plasmid. We acknowledge the support of this work by the National Institutes of Health (The Eunice Kennedy Shriver National Institute of Child Health and Human Development award HD078678).

Competing financial interests: The authors declare that they have no competing financial interests.

References

1. Nedergaard, M., Ransom, B., Goldman, S.A. (2003). New roles for astrocytes: redefining the functional architecture of the brain. *Trends in neurosciences* **26**, 523-530.
2. Parpura, V., Verkhratsky, A. (2012). Homeostatic function of astrocytes: Ca(2+) and Na(+) signalling. *Translational neuroscience* **3**, 334-344.
3. Hynd, M. R., Scott, H. L., Dodd P. R. (2004). Glutamate-mediated excitotoxicity and neurodegeneration in Alzheimer's disease. *Neurochemistry international* **45**, 583-595.
4. Danbolt, N. C. (2001). Glutamate uptake. *Progress in neurobiology* **65**, 1-105.
5. Hertz, L., Dringen, R., Schousboe, A., Robinson, S. R. (1999). Astrocytes: glutamate producers for neurons. *Journal of neuroscience research* **57**, 417-428.
6. Potokar, M., Kreft, M., Li, L., Daniel Andersson, J., Pangrsic, T., Chowdhury, H. H., Pekny, M., Zorec R. (2007). Cytoskeleton and vesicle mobility in astrocytes. *Traffic* **8**, 12-20.
7. Kreft, M., Potokar, M., Stenovec, M., Pangrsic, T., Zorec, R. (2009). Regulated exocytosis and vesicle trafficking in astrocytes. *Annals of the New York Academy of Sciences* **1152**, 30-42.
8. Potokar, M., Kreft, M., Pangrsic, T., Zorec, R. (2005). Vesicle mobility studied in cultured astrocytes. *Biochemical and biophysical research communications* **329**, 678-683.
9. Osborne, K. D., Lee, W., Malarkey, E. B., Irving, A. J., Parpura, V. (2009). Dynamic imaging of cannabinoid receptor 1 vesicular trafficking in cultured astrocytes. *ASN neuro* **1**, 283-296.
10. Reyes, R. C., Perry, G., Lesort, M., Parpura, V. (2011). Immunophilin deficiency augments Ca2+-dependent glutamate release from mouse cortical astrocytes. *Cell Calcium* **49**, 23-34.
11. Gottipati, M. K., Kalinina, I., Bekyarova, E., Haddon, R. C., Parpura, V. (2012). Chemically functionalized water-soluble single-walled carbon nanotubes modulate morpho-functional characteristics of astrocytes. *Nano letters* **12**, 4742-4747.
12. McCarthy, K. D., de Vellis, J. (1980). Preparation of separate astroglial and oligodendroglial cell cultures from rat cerebral tissue. *The Journal of cell biology* **85**, 890-902.
13. Lee, W., Parpura, V. (2012). Dissociated cell culture for testing effects of carbon nanotubes on neuronal growth. *Methods Mol Biol* **846**, 261-276.
14. Malarkey, E. B., Parpura, V. (2011). Temporal characteristics of vesicular fusion in astrocytes: examination of synaptobrevin 2-laden vesicles at single vesicle resolution. *The Journal of physiology* **589**, 4271-4300.
15. Haydon, P. G., Lartius, R., Parpura, V., Marchese-Ragona, S. P. (1996). Membrane deformation of living glial cells using atomic force microscopy. *Journal of microscopy* **182**, 114-120.